

## Overcoming the Circular Problem for $\gamma$ -ray Bursts in Cosmological Global Fitting Analysis

Hong Li<sup>1</sup>, Jun-Qing Xia<sup>2</sup>, Jie Liu<sup>2</sup>, Gong-Bo Zhao<sup>3</sup>, Zu-Hui Fan<sup>1</sup> & Xinmin Zhang<sup>2</sup>

### ABSTRACT

Due to the lack of low redshift long Gamma-Ray Bursts (GRBs), the circular problem has been a severe obstacle for using GRBs as cosmological candles. In this paper, we present a new method to deal with such a problem in Markov Chain Monte Carlo (MCMC) global fitting analysis. Our methodology is similar to that of self-calibrations in using clusters of galaxies as cosmological probes. Assuming that a certain type of correlations between different observables exists in a subsample of GRBs, for the parameters involved in the correlation relation, we treat them as free parameters and determine them simultaneously with cosmological parameters through MCMC analysis on GRB data together with other observational data, such as SNe Ia, cosmic microwave background radiation (CMB) and large-scale structure (LSS). Then the circular problem is naturally eliminated in this procedure. To demonstrate the feasibility of our method, we take the Ghirlanda relation ( $E_\gamma \propto CE_{\text{peak}}^A$ ) as an example while keeping in mind the debate about its physical validity. Together with SNe Ia, WMAP and SDSS data, we include 27 GRBs with the reported Ghirlanda relation in our study, and perform MCMC global fitting. We consider the  $\Lambda$ CDM model and dynamical dark energy models with equation of state (EoS)  $w_{\text{DE}} = w_0 + w_1(1 - a)$  and the oscillating EoS  $w_{\text{DE}} = w_0 + w_1 \sin(w_2 \ln(a))$ , respectively. We also include the curvature of the universe in our analysis. In each case, in addition to the constraints on the relevant cosmological parameters, we obtain the best fit values as well as the distributions of the correlation parameters  $A$  and  $C$ . We find that the observational data sets other than GRBs can affect  $A$  and  $C$  considerably through their degeneracies with the cosmological parameters. With CMB+LSS+SNe+GRB data included in the analysis, the results on  $A$  and  $C$  for different cosmological models are in well agreement within  $1\sigma$  range. The best fit value of  $A$  in all models being analyzed is  $A \sim 1.53$  with  $\sigma \sim 0.08$ . For  $C$ , we have the best value in the range of  $0.94 - 0.98$  with  $\sigma \sim 0.1$ . It is also noted

---

<sup>1</sup>Department of Astronomy, School of Physics, Peking University, Beijing, 100871, P. R. China.

<sup>2</sup>Institute of High Energy Physics, Chinese Academy of Science, P. O. Box 918-4, Beijing 100049, P. R. China;  
Email Address: xiajq@mail.ihep.ac.cn.

<sup>3</sup>Department of Physics, Simon Fraser University, Burnaby, BC, V5A 1S6, Canada.

that the distributions of  $A$  and  $C$  are generally broader than the priors used in many studies in literature. Our method can be readily applied to other GRB relations, which might be better physically motivated.

*Subject headings:* Cosmological Parameters – Cosmology: Observations – Gamma-rays: Bursts

## 1. Introduction

Searching for the nature of dark energy has been one of the most challenging tasks in cosmological studies. Because of the existence of degeneracies between dark energy parameters and the other cosmological parameters in different observables, multi-probe analysis are essential in constraining tightly the properties of dark energy. In this regard, exploring new probes has its great importance. On the other hand, thorough investigations on different probes both observationally and theoretically are equally important so that we can understand their validity and limitations in cosmological applications.

GRBs are the most powerful events observed in the cosmos, and can potentially be used to probe the high-redshift universe. Recently, several empirical correlations between GRB observables were reported, which have triggered intensive studies on the possibility in using GRBs as cosmological known candles (Norris et al. (2000), Lloyd-Ronning & Ramirez-Ruiz (2002), Ghirlanda et al. (2004a), Ghirlanda et al. (2004b), Dai et al. (2004), Xu et al. (2005), Firmani et al. (2005), Friedman & Bloom (2005), Firmani et al. (2006), Schaefer (2007)). Constraints on cosmological parameters from GRBs alone and in conjunction with other geometrical probes, including SNe Ia, the shift parameter from CMB measurements (Wang & Mukherjee (2006)) and the  $A$  parameter for the signals of baryon acoustic oscillation (BAO) from galaxy redshift surveys (Eisenstein et al. (2005)), have been analyzed (Su et al. (2006), Wright (2007), Wang et al. (2007)). Li et al. (2008), for the first time, performed global fitting on the GRB data with the MCMC technique together with SNe Ia data (Riess et al. (2007)), and data from WMAP (Spergel et al. (2007)), SDSS (Tegmark et al. (2004)) and 2dFGRS (Cole et al. (2005)). On the other hand, the physics behind the empirical correlations are poorly understood. There are also observational indications that some of the reported correlations may have potential problems. Thus there is an ongoing debate for the validity of using GRBs as cosmological candles. The circular problem has been recognized as another obstacle in the cosmological applications of GRBs. Up to now, there have been about 100 GRBs with measured redshifts, and few are at low redshifts with known distances. Thus it is lack of observational data to calibrate, in a cosmology-independent way, the correlation relations. The reported relations are often given assuming an input cosmology. Applying such relations to constrain cosmological parameters leads to the circular problem. Different methods have been put

forward to avoid this problem (Firmani et al. (2005), Schaefer (2007)). All of them are discussed in the context of using geometrical constraints only.

In this paper, we present a method to deal with the circular problem in the MCMC global fitting. It is known that for constraining cosmological parameters, the most reliable way is to perform global fitting from observational data directly. Li et al. (2008) made a first effort to integrate GRBs in the MCMC chains. However, the GRB data they used are released by Schaefer (2007) where the distance moduli of GRB samples are not independent of the input cosmology model and are still subject to the circular problem. Due to this reason, here we aim at introducing a new method to get rid of the circular problem of GRBs in order to avoid biases arising from it, so that the advantage of the MCMC global fitting can be fully realized. We are aware of the current debate regarding the cosmological applicability of GRBs (Bloom et al. (2003), Friedman & Bloom (2005)). On the other hand, with both observational and theoretical advances, reliable correlation relations from sub classes of GRBs may eventually emerge. With these considerations in mind, we have made our method as general as possible. It is not limited to any specific correlations. However, to demonstrate its feasibility, we have to work on a concrete example. We choose the Ghirlanda relation (Firmani et al. (2006)) in our present study. Our method can be readily applied to other correlations. The cosmological models to be analyzed include the  $\Lambda$ CDM model and dynamical dark energy models with the EoS following  $w_{\text{DE}} = w_0 + w_1(1 - a)$  and  $w_{\text{DE}} = w_0 + w_1 \sin(w_2 \ln(a))$ , respectively. The dark energy perturbations are fully taken into account.

## 2. Methodology

For the paper to be self-contained, in this section, we firstly describe briefly the Ghirlanda relation, and then we present our analyzing method dealing with the circular problem of GRBs in the MCMC fitting procedure. The general global fitting procedure will be explained in the second part of the section.

### 2.1. The Ghirlanda relation and the method

Keeping in mind its general applicability, we have to choose a specific correlation for GRBs as an example to show quantitatively the feasibility of our method in the MCMC global fitting analysis. Among the reported correlations, the Ghirlanda relation is the one that has been used most extensively in constraining cosmology due to its relatively small scatters and the relatively large number of data points available. Recently, there have been intensive arguments questioning this relation largely because of the observed complexities of the X-ray light curves, which lead to

the difficulties in identifying jet break features. On the other hand, it has been pointed out that the X-ray and the optical emissions of GRB afterglows may have different origins, and thus can behave differently. In the recent study of Ghirlanda et al. (2007), they emphasize that the jet break features should be considered only if they appear in optical light curves. With the awareness of these debates, we here adopt the Ghirlanda relation in our analysis, and focus on the method for the circular problem, instead of on the cosmological constraints from GRB data.

The Ghirlanda relation, or the  $E_{\text{peak}} - E_{\gamma}$  correlation, relies on the jet break feature to calculate the jet opening angle  $\theta_{\text{jet}}$ , which, in turn, is crucial in correcting the GRB prompt emission energy for the collimation effects. Here we adopt the homogeneous medium model with

$$\theta_{\text{jet}} = 0.161 \left( \frac{t_{j,d}}{1+z} \right)^{3/8} \left( \frac{n_0 \eta_{\gamma}}{E_{\text{iso},52}} \right)^{1/8}, \quad (1)$$

where  $z$  is the redshift,  $\eta_{\gamma}$  is the radiative efficiency,  $t_{j,d}$  is the break time in days with  $t_{j,d} = t_j/1 \text{ day}$ ,  $n_0$  is the number density of particles in the surrounding interstellar medium with  $n_0 = n/1 \text{ cm}^{-3}$  and  $E_{\text{iso}}$  is the isotropic-equivalent energy of GRBs with  $E_{\text{iso},52} = E_{\text{iso}}/10^{52} \text{ ergs}$ . The quantity  $E_{\text{iso}}$  is related to the observed fluence  $S_{\gamma}$  in units of  $\text{erg/cm}^2$  as follows:

$$E_{\text{iso}} = \frac{4\pi d_L^2 S_{\gamma} k}{1+z}, \quad (2)$$

where  $d_L$  is the luminosity distance at redshift  $z$ , and  $k$  is a multiplicative correction related the observed bandpass to a standard rest-frame bandpass ( $1-10^4 \text{ keV}$  in this paper) (Bloom et al. (2001)). The collimation corrected energy  $E_{\gamma}$  is

$$E_{\gamma} = (1 - \cos \theta_{\text{jet}}) E_{\text{iso}}. \quad (3)$$

Following Xu et al. (2005), we write the  $E_{\text{peak}} - E_{\gamma}$  correlation in the following form:

$$\frac{E_{\gamma}}{10^{50} \text{ ergs}} = C \left( \frac{E_{\text{peak}}}{100 \text{ keV}} \right)^A, \quad (4)$$

where the parameters  $A$  and  $C$  are assumed to be constant, and  $E_{\text{peak}} = E_{\text{peak}}^{\text{obs}} (1+z)$ . It is seen that besides the direct observables, the luminosity distance  $d_L$  comes in through Eqs.(1-2). If, for a set of GRBs, their distances can be determined independently, one can calibrate the correlation relation (4) and find the values of  $A$  and  $C$  from observations directly. Then the cosmology-independent correlation can be used to estimate  $d_L$  for other GRBs and further to constrain cosmology. Unfortunately we lack of GRBs with known distances. Therefore in order to obtain values of  $A$  and  $C$ , one has to assume a cosmological model to calculate  $d_L$ . The circular problem arises when the luminosity distances derived from such a cosmology-dependent correlation relation are used

as cosmological candles. Different methods have been discussed to avoid the circular problem in grid-based  $\chi^2$  analysis involving only geometrical probes. In the following we describe our method to deal with the circular problem in MCMC global fitting procedures.

The essential of our method is that for an assumed functional form of a correlation relation such as in Eq.(4), we set the correlation parameters free in our analyzing process instead of using the values reported in other studies. Simultaneously with the cosmological parameters, their values are determined through global fittings with GRB data and other data sets, including CMB, LSS and SNe. Specifically, for each element on MCMC chains with a set of parameters  $(x_i, A, C)$ , where  $x_i$ ,  $i = 1 \cdots n$  are cosmological parameters we are interested in, the ‘‘observed’’ luminosity distance for each GRB is obtained through Eqs.(1-4) as:

$$d_L = 7.575 \frac{(1+z)C^{2/3}[E_{\text{peak}}^{\text{obs}}(1+z)/100 \text{ keV}]^{2A/3}}{(kS_\gamma t_{j,d})^{1/2}(n_0\eta_\gamma)^{1/6}} \text{ Mpc} , \quad (5)$$

where the small angle approximation with  $\theta_{\text{jet}} \ll 1$  has been applied. With the assumption that all the GRB observables are independent of each other with gaussian distributed errors, the uncertainty for each of these ‘‘data’’ points is estimated as follows (Friedman & Bloom (2005))

$$\begin{aligned} \left(\frac{\sigma_{d_L}}{d_L}\right)^2 &= \frac{1}{4} \left[ \left(\frac{\sigma_{S_\gamma}}{S_\gamma}\right)^2 + \left(\frac{\sigma_k}{k}\right)^2 \right] + \frac{1}{4} \frac{1}{(1 - \sqrt{C_\theta})^2} \left( A \frac{\sigma_{E_{\text{peak}}^{\text{obs}}}}{E_{\text{peak}}^{\text{obs}}} \right)^2 \\ &+ \frac{1}{4} \frac{C_\theta}{(1 - \sqrt{C_\theta})^2} \left[ \left(\frac{3\sigma_{t_{j,d}}}{t_{j,d}}\right)^2 + \left(\frac{\sigma_{n_0}}{n_0}\right)^2 + \left(\frac{\sigma_{\eta_\gamma}}{\eta_\gamma}\right)^2 \right] , \end{aligned} \quad (6)$$

where

$$C_\theta = [\theta \sin \theta / (8 - 8 \cos \theta)]^2 . \quad (7)$$

We take  $\eta_\gamma = 0.2$  and  $\sigma_{\eta_\gamma} = 0$  throughout this paper (Frail et al. (2001)). It is noted that when Eq.(6) is used to calculate  $\sigma_{d_L}$ , it is implicitly assumed that the correlation Eq.(4) has no additional scatters besides the uncertainties for the parameters  $A$  and  $C$ . Considering the distance modulus, we have

$$\mu_{\text{obs}} = 5 \log_{10} d_L + 25 , \quad (8)$$

and

$$\sigma_{\mu_{\text{obs}}} = \frac{5}{\ln 10} \left( \frac{\sigma_{d_L}}{d_L} \right) . \quad (9)$$

In order to constrain the cosmological parameters  $x_i$ , we have marginalized the free parameters  $A$  and  $C$ , and finally we get the probability for a certain cosmological parameter  $x_i$  as follows:

$$P(x_i) = \int P(x_i|x_j \cdots A, C)P(x_j) \cdots P(A)P(C)dx_j \cdots dAdC , \quad (10)$$

which are related to  $\chi^2$  given by the statistic results of the observational data via  $P \propto e^{-\chi^2/2}$ . And the  $\chi^2$  contributed by GRB “data” at the point  $(x_i, A, C)$  is then computed as

$$\chi^2(x_i, A, C) = \sum \left[ \frac{\mu_{\text{th}}(x_i) - \mu_{\text{obs}}(x_i, A, C)}{\sigma_{\mu_{\text{obs}}}} \right]^2, \quad (11)$$

where the summation is over the number of GRB data points.

We use 27 GRBs, which are reportedly to satisfy the  $E_{\text{peak}} - E_{\gamma}$  relation, in our study. The relevant data are listed in Table 1. In Table 1, the data are mostly from Ghirlanda et al. (2007) except for GRB050505 and GRB060210. For these two GRBs, we take the data from Schaefer (2007)<sup>4</sup>.

## 2.2. Global fitting program

Different observations play complementary roles in the determination of cosmological parameters. Their combination can effectively break out the degeneracies between different parameters, and therefore can deliver much better constraints on cosmology than any single probe can. For different observable, it is important to understand the main factors that affect the determination of interested parameters. The information on these elements extracted from observational data is very useful. Under certain conditions, the extracted values of these factors can be used to probe cosmology without invoking complicated observational data, which could greatly simplify the analyzing procedures. The two important examples are the shift parameter from CMB observations and the BAO  $A$  parameter from galaxy redshift surveys, and they have been widely used in constraining properties of dark energy. On the other hand, however, careful attentions must be paid to the conditions under which the extracted information is obtained. Inappropriate using of these pieces of information can lead to biased conclusions on the values of cosmological parameters. Therefore the most reliable way in determining cosmology is to perform global fitting analysis using observational data directly. Our global fitting analysis are based on the publicly available MCMC package CosmoMC (Lewis & Bridle (2002)). We have made modifications according to our own research purposes. Besides the modifications described in part A of this section, which are specific for the circular problem of GRBs, we include dark energy perturbations in our general analyzing program.

For dark energy models with equation of state  $w \neq -1$ , the perturbations inevitably exist. While the effects of dark energy perturbations are yet to be fully explored, it is generally believed that they may only show their influences at near-horizon scales. For CMB anisotropy, the

---

<sup>4</sup>Communications with Ghirlanda, 2007.

Table 1: Sample of 27 GRBs

GRB	$z$	$E_{\text{peak}}^{\text{obs}} (\sigma_{E_{\text{peak}}^{\text{obs}}})$ (keV)	$S_{\gamma} (\sigma_{S_{\gamma}})$ ( $10^{-6} \text{ ergs/cm}^2$ )	$t_{j,d} (\sigma_{t_{j,d}})$ (days)	${}^a n (\sigma_n)$ ( $\text{cm}^{-3}$ )	${}^b$ Reference ( $z, E_{\text{peak}}^{\text{obs}}, S_{\gamma}, t_{j,d}, n$ )
970828	0.9578	297.7 [59.5]	96.0 [9.6]	2.2 [0.4]	3.0 [2.4]	01,28,41,01,no
980703	0.966	254 [50.8]	22.6 [2.3]	3.4 [0.5]	28.0 [10.0]	02,28,41,48,48
990123	1.600	780.8 [61.9]	300 [40]	2.04 [0.46]	3.0 [2.4]	03,29,29,49,no
990510	1.619	161.5 [16.1]	19 [2]	1.6 [0.2]	0.29 [0.14]	04,29,29,50,68
990705	0.8424	188.8 [15.2]	75 [8]	1.0 [0.2]	3.0 [2.4]	05,29,29,51,no
990712	0.4331	65 [11]	6.5 [0.3]	1.6 [0.2]	3.0 [2.4]	06,29,29,52,no
991216	1.020	317.3 [63.4]	194 [19]	1.2 [0.4]	4.7 [2.8]	07,28,41,53,68
010222	1.480	309 [12]	93 [3]	0.93 [0.1]	3.0 [2.4]	08,29,42,54,no
011211	2.140	59.2 [7.6]	5.0 [0.5]	1.56 [0.02]	3.0 [2.4]	09,30,41,55,no
020124	3.200	120.0 [22.6]	6.8 [0.68]	3.0 [0.4]	3.0 [2.4]	10,31,31,56,no
020405	0.690	192.5 [53.8]	74 [0.7]	1.67 [0.52]	3.0 [2.4]	11,32,32,32,no
020813	1.255	142 [13]	97.9 [10]	0.43 [0.06]	3.0 [2.4]	12,31,31,57,no
021004	2.332	79.8 [30]	2.6 [0.6]	4.74 [0.14]	30.0 [27.0]	13,33,33,58,69
021211	1.006	46.8 [5.5]	3.5 [0.1]	1.4 [0.5]	3.0 [2.4]	14,34,34,59,no
030226	1.986	97 [20]	5.61 [0.65]	1.04 [0.12]	3.0 [2.4]	15,33,33,60,no
030328	1.520	130.2 [13.9]	37 [1.4]	0.8 [0.1]	3.0 [2.4]	16,33,33,61,no
030329	0.1685	67.9 [2.2]	163 [10]	0.5 [0.1]	1.0 [0.11]	17,35,35,62,70
030429	2.6564	35 [9]	0.85 [0.14]	1.77 [1]	3.0 [2.4]	18,33,33,18,no
041006	0.716	63.4 [12.7]	19.9 [1.99]	0.16 [0.04]	3.0 [2.4]	19,36,43,63,no
050401	2.900	128.5 [30]	19.3 [0.4]	1.5 [0.5]	3.0 [2.4]	20,37,40,27,no
050416	0.653	17.3 [5]	0.35 [0.03]	1.0 [0.7]	3.0 [2.4]	21,38,40,27,no
050505	4.270	70 $^{+140}_{-24}$	4.1 [0.4]	0.21 [0.04]	3.0 [2.4]	22,39,44,64,no
050525	0.606	79 [3.5]	20.1 [0.5]	0.28 [0.12]	3.0 [2.4]	23,37,45,65,no
050820	2.612	246 $^{+76}_{-40}$	52.7 [6.9]	15.2 [8]	3.0 [2.4]	24,37,40,27,no
060210	3.910	149 $^{+400}_{-35}$	7.7 [0.4]	0.33 [0.08]	3.0 [2.4]	25,40,46,66,no
060526	3.210	24.94 [5]	0.49 [0.06]	2.77 [0.3]	3.0 [2.4]	26,40,47,67,no
060614	0.125	48.9 [40]	21.7 [0.4]	1.38 [0.04]	3.0 [2.4]	27,27,27,27,no

<sup>a</sup>The circumburst densities and errors from broadband modelling of the afterglow light curves. If no available the value of  $n$  is taken as  $3.0 \pm 2.4 \text{ cm}^{-3}$ .

<sup>b</sup>References for the GRBs data in the table: (01) Djorgovski, S. G. et al. 2001, ApJ, 562, 654; (02) Djorgovski, S.G. et al. 1998, ApJ, 508, L17; (03) Kulkarni, S. R. et al. 1999, Nature, 398, 389; (04) Vreeswijk, P. M. et al. 2001, ApJ, 546, 672; (05) Le Floch, E. 2002, ApJ, 581, L81; (06) Vreeswijk, P. M. et al. 2001, ApJ, 546, 672; (07) Piro, L. et al. 2000, Science, 290, 955; (08) Fruchter, A. et al. 2001a, GCN 1029; (09) Holland, et al. 2002, AJ, 124, 639; (10) Hjorth, J. et al. 2003, ApJ, 597, 699; (11) Price, P. A. et al. 2003a, ApJ, 589, 838; (12) Barth, A. J. et al. 2003, ApJ, 584, L47; (13) Matheson, T. et al. 2003, ApJ, 582, L5; (14) Vreeswijk, P. M. et al. 2003, GCN, 1785; (15) Greiner, J. et al. 2003a, GCN, 1886; (16) Rol, E. et al. 2003, GCN, 1981; (17) Greiner, J. et al. 2003b, GCN, 2020; (18) Jakobsson, P. et al. 2004, A&A, 427, 785; (19) Fugazza, D. et al. 2004, GCN 2782; (20) Fynbo, J. P. U. et al. 2005b, GCN 3176; (21) Cenko, S. B. et al. 2005, GCN 3542; (22) Berger, E. et al. 2005b, GCN 3368; (23) Foley, R. J. et al. 2005, GCN 3483; (24) Prochaska, J. X. et al. 2005b, GCN 3833; (25) Cucchiara, A. et al. 2006a, GCN 4729; (26) Berger, E. & Gladders, M. 2006, GCN 5170; (27) G. Ghirlanda, L. Nava, G. Ghisellini and C. Firmani, astro-ph/0702352; (28) Jimenez, R., Band, D. L., & Piran, T., 2001, ApJ, 561, 171; (29) Amati, L. et al. 2002, A&A, 390, 81; (30) Amati, L. 2004, astro-ph/0405318; (31) Barraud, C. et al. 2003, A&A, 400, 1021; (32) Price, P. A. et al. 2003a, ApJ, 589, 838; (33) Sakamoto, T. et al., 2004b, astro-ph/0409128; (34) Crew, G. B. et al. 2003, ApJ, 599, 387; (35) Vanderspek, R. et al. 2004, AJ, 617, 1251; (36) HETE 2006, <http://space.mit.edu/HETE/Bursts/>; (37) Krimm, H. et al. 2006a, in Gamma-Ray Bursts in the Swift Era, eds S. S. Holt, N. Gehrels, and J. A. Nousek (AIP Conf. Proc. 836), pp. 145-148; (38) Sakamoto, T. et al. 2006b, ApJ, 636, L73; (39) Krimm, H. et al. 2005, GCN 3134; (40) Schaefer, astro-ph/0612285; (41) Bloom, J. S., Frail, D. A., & Kulkarni, S. R. 2003, ApJ, 594, 674; (42) Frontera, F. et al. 2001, GCN 1215; (43) Galassi, M. et al. 2004, GCN 2770; (44) Hullinger, D. et al. 2005, GCN 3364; (45) Cummings, J. et al. 2005, GCN 3479; (46) Sakamoto, T. et al. 2006d, GCN 4748; (47) Markwardt, C. et al. 2006, GCN 5174; (48) Frail, D. A. et al. 2003, ApJ, 590, 992; (49) Kulkarni, S. R. et al. 1999, Nature, 398, 389; (50) Stanek, K. Z. et al. 1999, ApJ, 522, L39; (51) Masetti, N. et al. 2000, A&A, 354, 473; (52) Björnsson G. et al. 2001, ApJ, 552, L121; (53) Halpern, J. P., et al. 2000, ApJ, 543, 697; (54) Jakobsson, P. et al. 2003, A&A, 408, 941; (55) Jakobsson, P. et al. 2003, A&A, 408, 941; (56) Berger, E. et al. 2002, ApJ, 581, 981; (57) Barth, A. J. et al. 2003, ApJ, 584, L47; (58) Holland, et al. 2003, AJ, 125, 2291; (59) Holland, et al. 2004, astro-ph/0405062; (60) Klose, S. et al. 2004, AJ, 128, 1942; (61) Andersen, M. I. et al. 2003, GCN, 1993; (62) Price, P. A. et al. 2003b, Nature, 423, 844; (63) Stanek, K. Z. et al. 2005, ApJ, 626, L5; (64) Hurkett, C. P. et al. 2006, MNRAS, 368, 1101; (65) Blustin, A. J. et al. 2006, ApJ, 637, 901; (66) Dai, X. & Stanek, Z. 2006, GCN 5147; (67) Moretti, A. et al. 2006, GCN 5194; (68) Panaitescu, A., & Kumar, P. 2002, ApJ, 571, 779; (69) Schaefer, B. E. 2003, ApJ, 583, L67 (S03); (70) Tiengo, A. et al. 2003, A&A, 409, 938.

power spectrum at low  $l$  (large angular scale) is affected by the late Integrated Sachs-Wolfe Effect (ISW), whose strength depends on the properties of dark energy in a flat universe. Thus large-scale anisotropy is important and the perturbations can play roles in dark energy studies. It is well recognized that in the fluid approach, there is a divergence problem at  $w = -1$  when dark energy perturbations are included. On the other hand, there are observational indications that the equation of state of dark energy may cross  $-1$  during the evolutionary history of the universe (Huterer & Cooray (2005), Feng et al. (2005), Xia et al. (2006), Zhao et al. (2007a)). Thus for dark energy perturbations, the divergence problem must be carefully dealt with. From our analysis on two-field quintom models (Feng et al. (2005), Zhang et al. (2006)), in which  $w$  crosses  $-1$  can be realized, we find that the dark energy perturbations are well behaved at  $w = -1$ . Thus the divergence in the fluid treatment should be a mathematical one instead of a physical one. Along this line of thinking, we develop a scheme in the fluid approach to avoid the divergence problem (Zhao et al. (2005), Xia et al. (2006)).

In the conformal Newtonian gauge, the perturbation equations of dark energy are:

$$\dot{\delta} = -(1+w)(\theta - 3\dot{\Phi}) - 3\mathcal{H}(c_s^2 - w)\delta, \quad (12)$$

$$\dot{\theta} = -\mathcal{H}(1-3w)\theta - \frac{\dot{w}}{1+w}\theta + k^2\left(\frac{c_s^2\delta}{1+w} + \Psi\right). \quad (13)$$

where  $\delta$  and  $\theta$  are the energy density and velocity perturbations, respectively. The divergence at  $w = -1$  can be seen from the second equation. To handle this problem, we introduce a small constant  $\epsilon$ , and divid  $w$  into three parts with 1)  $w > -1 + \epsilon$ ; 2)  $-1 + \epsilon \geq w \geq -1 - \epsilon$ ; and 3)  $w < -1 - \epsilon$ , respectively. For regions 1) and 3), the perturbations are analyzed following the equations. For region 2), we need a special treatment. We match the perturbation quantities of region 2) to regions 1) and 3) at the corresponding boundaries, and set

$$\dot{\delta} = 0, \quad \dot{\theta} = 0. \quad (14)$$

within the region. Thus there are discontinuities in the derivatives in region 2). But with small enough  $\epsilon$ , the discontinuities have negligible effects. We compare the results from this analysis with those of two-field quintom models and find that with  $\epsilon \leq 10^{-5}$ , the perturbations of the quintom models can well be reproduced by this fluid approach. For more details of this method we refer the readers to our previous companion papers (Zhao et al. (2005), Xia et al. (2006)). Thus we set  $\epsilon = 10^{-5}$  in our studies.

We consider three cosmological models, the  $\Lambda$ CDM model including the curvature term, and dynamical dark energy models with the equation of state parameterized respectively as

$$\text{I)} \quad w_{\text{DE}}(a) = w_0 + w_1(1-a), \quad (15)$$

$$\text{II)} \quad w_{\text{DE}}(a) = w_0 + w_1 \sin(w_2 \ln(a)), \quad (16)$$



where  $a = 1/(1 + z)$  is the scale factor and  $w_1$  characterizes the “running” of the EoS. For the parametrization I (Para I), we include the curvature term. In the parametrization II (Para II), we are limited in the flat universe and fix  $w_2 = 3\pi/2$  for not introducing too many parameters during the fitting process.

Our most general parameter space is then:

$$\mathbf{P} \equiv (\omega_b, \omega_c, \Omega_K, \Theta_s, \tau, w_0, w_1, n_s, \ln(10^{10} A_s), A, C) \quad (17)$$

where  $\omega_b \equiv \Omega_b h^2$ ,  $\omega_c \equiv \Omega_c h^2$ ,  $\Omega_K$  represents the contribution of the curvature term to the total energy budget,  $\Theta_s$  is the ratio (multiplied by 100) of the sound horizon at decoupling to the angular diameter distance to the last scattering surface,  $\tau$  is the optical depth due to re-ionization,  $w_0$  and  $w_1$  is the parameters of the EoS of Dark Energy,  $A_s$  and  $n_s$  characterize the power spectrum of primordial scalar perturbations,  $A$  and  $C$  are the free parameters related to the  $E_{\text{peak}} - E_\gamma$  correlation. For the  $\Lambda$ CDM models,  $w_0 = -1$ ,  $w_1 = 0$ .

We vary the above parameters and fit to the observational data with the MCMC method. For the pivot of the primordial spectrum we set  $k_{s0} = 0.05 \text{Mpc}^{-1}$ . The following weak priors are taken:  $\tau < 0.8$ ,  $0.5 < n_s < 1.5$ ,  $-3 < w_0 < 3$ ,  $-5 < w_1 < 5$ ,  $0.5 < A < 2.5$  and  $0.01 < C < 2.5$ . We impose a tophat prior on the cosmic age as  $10 \text{Gyr} < t_0 < 20 \text{Gyr}$ . Furthermore, we make use of the Hubble Space Telescope (HST) measurement of the Hubble parameter  $H_0 \equiv 100h \text{ km s}^{-1} \text{ Mpc}^{-1}$  by multiplying the likelihood by a Gaussian likelihood function centered around  $h = 0.72$  with a standard deviation  $\sigma = 0.08$  (Freedman et al. (2001)). We also adopt a Gaussian prior on the baryon density  $\Omega_b h^2 = 0.022 \pm 0.002$  ( $1\sigma$ ) from Big Bang Nucleosynthesis (Burles et al. (2001)).

In our calculations, we take the total likelihood to be the products of the separate likelihoods ( $\mathcal{L}_i$ ) of CMB, LSS, SNIa and GRBs. For CMB, we include the three-year WMAP (WMAP3) data and compute the likelihood with the routine supplied by the WMAP team (Spergel et al. (2007)). For the Large Scale Structure information, we have used the Sloan Digital Sky Survey (SDSS) luminous red galaxy (LRG) sample (Tegmark et al. (2006)). To minimize the nonlinear effects, we have only used the first 15 bins,  $0.0120 < k_{\text{eff}} < 0.0998$ , which are supposed to be well within the linear regime. For SNe Ia, we mainly present the results with the recently released *Essence* 192 sample supernovae published in Miknaitis et al. (2007) and Davis et al. (2007). In the calculation of the likelihood from SNe Ia data, we marginalize over the nuisance parameter (Goliath et al. (2001), Di Pietro & Claeskens (2003)).

For each regular calculation, we run 8 independent chains comprising of 150,000 – 300,000 chain elements, and spend thousands of CPU hours on a supercomputer. The average acceptance rate is about 40%. We test the convergence of the chains by Gelman and Rubin criteria (Gelman & Rubin (1992)) and find that  $R - 1$  is on the order of 0.01, which is much more conservative than the recommended value  $R - 1 < 0.1$ .

TABLE II. Constraints on the EoS of dark energy and some background parameters from the current observations with and without GRBs. Note that Para I and Para II represent  $w_{\text{DE}}(a) = w_0 + w_1(1 - a)$  and  $w_{\text{DE}}(a) = w_0 + w_1 \sin(3\pi/2 \ln(a))$  respectively. For the current constraints we have shown the mean values  $1\sigma$  (Mean).

	$\Lambda$ CDM		Para I		Para I + $\Omega_k$		Para II	
	GRB only	combined all	with GRB	without GRB	with GRB	without GRB	with GRB	without GRB
$w_0$	-1	-1	$-1.04^{+0.17}_{-0.16}$	$-1.01^{+0.18}_{-0.17}$	$-1.05 \pm 0.17$	$-1.02 \pm 0.17$	$-0.937^{+0.137}_{-0.147}$	$-0.968^{+0.148}_{-0.154}$
$w_1$	0	0	$0.344^{+0.641}_{-0.664}$	$0.192^{+0.741}_{-0.729}$	$0.273^{+0.723}_{-0.758}$	$0.228^{+0.728}_{-0.771}$	$0.016^{+0.187}_{-0.207}$	$-0.025^{+0.212}_{-0.221}$
$\Omega_{\text{DE}}$	$0.748^{+0.248}_{-0.748}$	$0.761 \pm 0.017$	$0.760 \pm 0.020$	$0.762 \pm 0.020$	$0.755 \pm 0.023$	$0.758 \pm 0.022$	$0.764^{+0.021}_{-0.020}$	$0.764^{+0.022}_{-0.021}$
$\Omega_k$	$-0.235^{+0.374}_{-0.347}$	0	0	0	$-0.002 \pm 0.014$	$0.001 \pm 0.014$	0	0
$A$	$1.51 \pm 0.0836$	$1.54^{+0.0782}_{-0.0768}$	$1.53^{+0.0781}_{-0.0758}$	0	$1.53^{+0.0771}_{-0.0769}$	0	$1.54^{+0.0774}_{-0.0736}$	0
$C$	$0.912^{+0.408}_{-0.352}$	$0.943^{+0.106}_{-0.108}$	$0.963 \pm 0.109$	0	$0.983^{+0.134}_{-0.139}$	0	$0.939^{+0.102}_{-0.0996}$	0

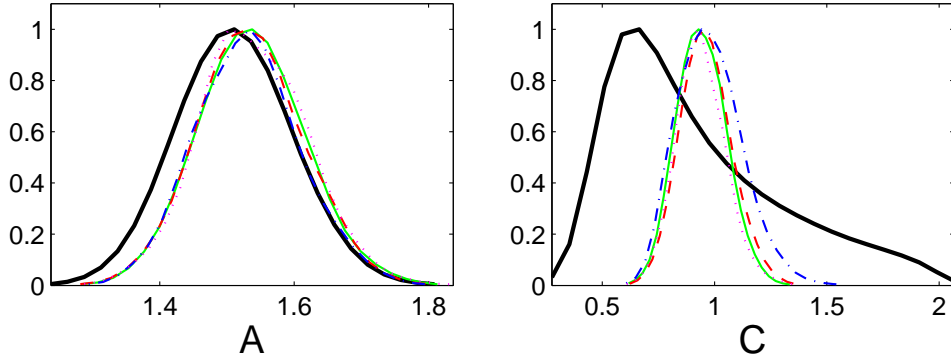


Fig. 1.— 1-d posterior constraints for the parameters  $A$  and  $C$  obtained via MCMC methods. The black solid lines are for the non-flat  $\Lambda$ CDM model using GRBs data only. The colored lines are the results from joint analysis of CMB+LSS+SNe+GRB. The green solid, red dashed, blue dash-dotted, and magenta dotted lines are for the  $\Lambda$ CDM, flat model with dark energy Para I, non-flat model with dark energy Para I, and flat model with dark energy Para II, respectively.

### 3. Results and Discussions

In this section, we present our main results. Firstly we consider the constraint on the non-flat  $\Lambda$ CDM model using GRB data only. In order to study the dependence of  $A$  and  $C$  on the cosmology models, we combine the GRB data with other cosmological observational data, such as CMB, LSS and SN, to constrain different dark energy models, namely the  $\Lambda$ CDM model and the dynamical dark energy models, Para I and Para II. Considering the degeneracy between the dark energy parameters and the curvature of universe (Zhao et al. (2007b), Clarkson et al. (2007)), we also consider the non-flat case in the dynamical dark energy model Para I. During these calculations, we focus on discussions of constraints on  $A$  and  $C$ , and the effects of GRB data on the determination of cosmological parameters.

In Figure 1, we show the one-point likelihood function for  $A$  and  $C$ , respectively. The black solid line in each panel represents the result for the non-flat  $\Lambda$ CDM model using GRB data only. The colored lines are the results from combined analysis of CMB+LSS+SNe+GRB for different cosmological models. The green solid, red dashed, blue dash-dotted, and magenta dotted lines are for the  $\Lambda$ CDM, flat model with dark energy parametrization I, non-flat model with dark energy Para I, and flat model with dark energy Para II, respectively.

It is immediately seen that through constraining the cosmological parameters, the data sets other than GRB have some effects on the likelihood of GRB parameters, especially on  $C$ . Both concerning the non-flat  $\Lambda$ CDM model, the black solid line in the right panel of Figure 1 is much broader than the green solid line. This is due to the degeneracy between the correlation parameters of GRB and the cosmological parameters. With GRB data only, cosmological parameters cannot be tightly constrained, and their large uncertainties in turn broaden the likelihood of  $C$ . Including other data sets greatly reduces the error ranges of cosmological parameters, resulting a much narrower likelihood distribution for  $C$ . It is also noted that the peak of the distribution of  $C$  shifts its position as well. This comparison clearly demonstrates the importance of our methodology in dealing with  $A$  and  $C$  and the importance of multi-probe analysis.

On the other hand, given the observational data sets, the dependence of  $A$  and  $C$  on cosmological models is rather weak, as seen from the results shown by the colored lines in Figure 1. The mean value of  $A$  in all four cosmological models is  $A \sim 1.53$  with  $1\sigma$  error about 0.08. For the parameter  $C$ , its variation for different cosmological models is slightly larger than that of  $A$ , with the average value of  $C = 0.94, 0.96, 0.98,$  and  $0.94$ , for the four models, respectively. They are in well agreement with each other within  $1\sigma$  range with  $\sigma \sim 0.1$ . Keeping in mind the hot debate regarding GRBs as cosmological candles due to the lack of thorough understanding of GRB physics and the quality of observational data, the consistency in  $A$  and  $C$  for different cosmological models seen from our global fitting analysis may hint that the Ghirlanda relation could be intrinsic to a subsample of GRBs.

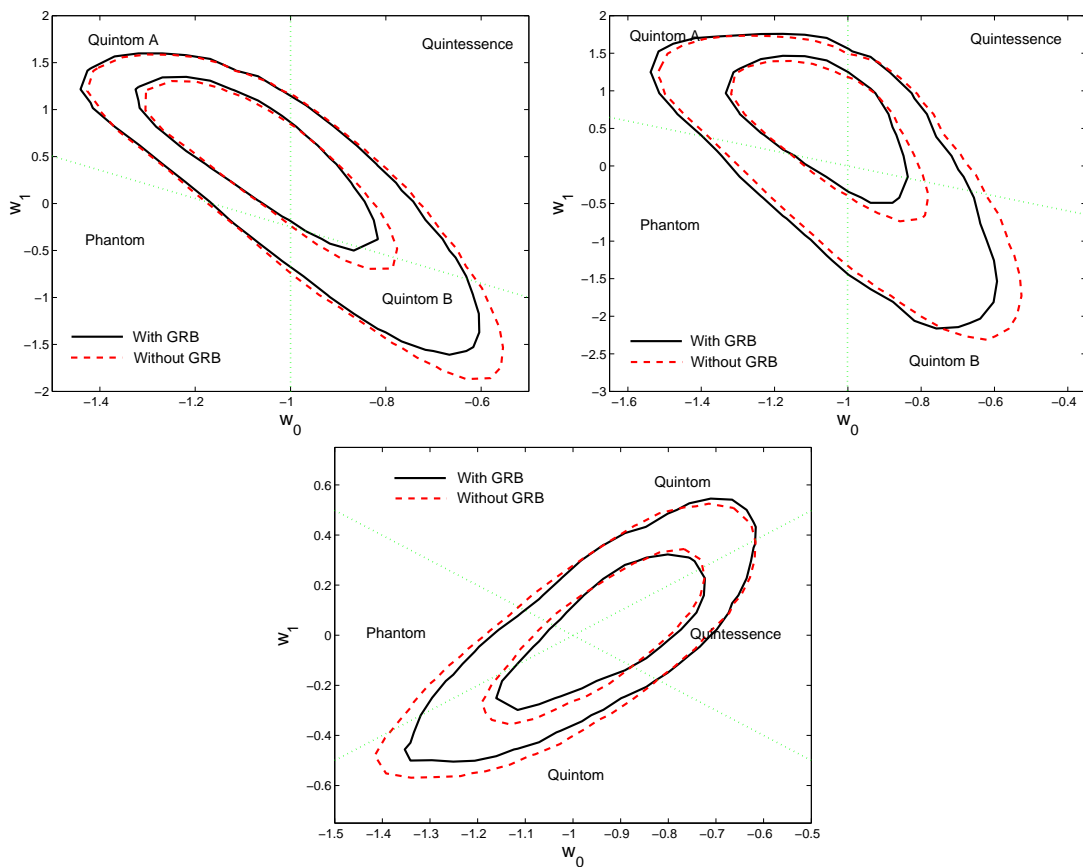


Fig. 2.— 2-d joint 68% and 95% confidence regions for the parameters  $w_0$  and  $w_1$  of flat model with dark energy Para I (first panel), non-flat model with dark energy Para I (second panel), and flat model with dark energy Para II (third panel), respectively. The black solid line is given by using WMAP3+SNIa+LSS+GRBs while the red dashed line comes from WMAP3+SNIa+LSS without GRBs. For both cases we considered the dark energy perturbation.

Because we determine  $A$  and  $C$  simultaneously with the cosmological parameters, their likelihood distributions shown in Figure 1 have included the effects of uncertain cosmology constrained by the current observational data. Therefore our global fitting analysis give a consistent evaluation on the contribution of GRBs to the determination of cosmological parameters. Both the distributions in  $A$  and  $C$  are broader than those estimated with a fixed cosmological model. Thus inappropriate use of the narrow uncertainties in  $A$  and  $C$  resulting from a given cosmology can lead to an overestimate of the power of GRBs in cosmological studies.

The results on the cosmological parameters constrained from our analysis are listed in Table II. In Figure 2, we show, respectively, the constraints on the dark energy parameters  $w_0 - w_1$  for the flat model with dark energy Para I (first panel), non-flat model with dark energy Para I (second panel), and flat model with dark energy Para II (third panel), respectively. The black solid and red dashed lines represent the results with and without the 27 GRBs included. For all the cases considered, the flat  $\Lambda$ CDM model is well consistent with the observational data with or without GRBs. For the case of flat model with Para I for the dark energy EoS, quintom A type of models with  $w_0 < -1$  and  $w_1 > 0$  are mildly favored by the data. Including the GRB data in the analysis, the  $1\sigma$  contour shifts more toward the quintom A region. Relaxing the strong prior on the flatness of the universe, the  $\Lambda$ CDM gives a better fit to the data than the above case. Considering the oscillating dark energy model, it is seen that the  $\Lambda$ CDM model with  $w_0 = -1$  and  $w_1 = 0$  is again in excellent agreement with the observational data. Comparing the black solid lines with the red dashed lines in Figure 2, we see some shrinkage of the error contours when including GRB data in the analysis, which is largely attributed to the high redshift range of GRBs. This indicates the possible potential in using GRBs as high-redshift cosmological candles. The contribution from the current GRB data is however not greatly significant. Nevertheless, given the apparent advantage of GRBs as the tracers of the high-redshift universe, it is important to perform detailed analysis as we did here to investigate their usefulness in cosmological studies.

#### 4. Summary

In this paper, we present a new method in dealing with the circular problem for GRBs in the determination of cosmological parameters. This method is implemented in our MCMC global fitting program. The methodology is to treat the parameters involved in a GRB correlation relation as free parameters when performing global fitting analysis. Their values are then simultaneously estimated together with the cosmological parameters we are interested in, and therefore the circular problem is naturally eliminated. Furthermore, our analysis can give the likelihood distributions of the correlation parameters with the uncertainties in the cosmological parameters being taken into account.

From the distributions of  $A$  and  $C$ , we can see that the dependence of  $A$  and  $C$  on the cosmology model is rather weak, and the constraints on  $A$  and  $C$  for different cosmological models are in well agreement within  $1\sigma$  range. However, the distributions of  $A$  and  $C$  are generally broader than the priors used in many studies in the literature which will lead to the overestimate of the power of GRBs in cosmological studies. With the combined datasets CMB+LSS+GRB+SNe, our global fitting results show that in different dynamical dark energy models the constraints on dark energy parameters become stringent by taking into account high redshift GRBs, which show the potential of GRBs in the cosmology studies.

We emphasize that our method can be readily applied to different correlation relations of GRBs although we take the Ghirlanda relation as a concrete example in this paper. In fact, the applicability of our method is even not limited to GRB studies. Any cosmological probe involving parameters other than cosmological ones can be analyzed with our method. Thus our implemented MCMC program presented in this paper can be a platform with wide applications. For example, in using the abundance of clusters of galaxies to constrain cosmology, the relations between direct observables, such as the X-ray brightness (temperature), the Sunyaev-Zel'dovich effect and the richness of galaxies, and the total mass of a cluster have to be involved. Applying the relations derived based on simplified assumptions regarding the physical state of clusters may lead to biased cosmological conclusions. It has been proposed to analyze such relations simultaneously with cosmological parameters to be studied. Our program is then perfectly suitable for such analysis.

It is noted that all our investigations and implementations are carried under the framework of MCMC global fitting using observational data directly. Therefore we can give more reliable estimates on the considered parameters than those of Fisher Matrix analysis or the constraints derived from some extracted parameters, such as the CMB shift parameter and the BAO parameter of large-scale structures of the universe.

Our MCMC chains were finished in the Sunway system of the Shanghai Supercomputer Center (SSC). We thank Zi-Gao Dai, Giancarlo Ghirlanda, Matteo Viel and Dong Xu for helpful discussions. This work is supported in part by China postdoctoral science foundation, National Science Foundation of China under Grant Nos. 90303004, 19925523, 10243006, 10373001, 10233010, 10221001 and 10533010, and by the Ministry of Science and Technology of China under Grant No. NKBRSF G19990754, TG1999075401 and the 973 program No.2007CB815401, and by the Key Grant Project of Chinese Ministry of Education (No. 305001). Gong-Bo Zhao is partly supported by the National Science and Engineering Research Council of Canada (NSERC).

## REFERENCES

- Bloom, J. S., Frail, D. A. & Sari, R. 2001, *AJ*, 121, 2879
- Bloom, J. S., Frail, D. A. & Kulkarni, S. R. 2003, *ApJ*, 594, 674
- Burles, S., Nollett, K. M. & Turner, M. S. 2001, *ApJ*, 552, L1
- Clarkson, C., Cortes, M. & Bassett, B. A. 2007, *JCAP*, 0708, 011
- Cole, S., et al. 2005, *MNRAS*, 362, 505
- Dai, Z. G., Liang, E. W. & Xu, D. 2004, *ApJ*, 612, L101
- Davis, T. M., et al. 2007, *ApJ*, 666, 716
- Di Pietro, E. & Claeskens, J. F. 2003, *MNRAS*, 341, 1299
- Eisenstein, D. J., et al. 2005, *ApJ*, 633, 560
- Feng, B., Wang, X. L. & Zhang, X. 2005, *Phys. Lett. B*, 607, 35
- Firmani, C., Ghisellini, G., Ghirlanda, G. & Avila-Reese, V. 2005, *MNRAS*, 360, L1
- Firmani, C., Ghisellini, G., Avila-Reese, V. & Ghirlanda, G. 2006, *MNRAS*, 370, 185
- Frail, D. A., et al. 2001, *ApJ*, 562, L55
- Freedman, W. L., et al. 2001, *ApJ*, 553, 47
- Friedman, A. S. & Bloom, J. S. 2005, *ApJ*, 627, 1
- Gelman, A. & Rubin, D. 1992, *Statistical Science*, 7, 457
- Ghirlanda, G., Ghisellini, G., Lazzati, D. & Firmani, C. 2004a, *ApJ*, 613, L13
- Ghirlanda, G., Ghisellini, G. & Lazzati, D. 2004b, *ApJ*, 616, 331
- Ghirlanda, G., Nava, L., Ghisellini, G. & Firmani, C. 2007, *A&A*, 466, 127
- Goliath, M., Amanullah, R., Astier, P., Goobar, A. & Pain, R. 2001, *A&A*, 380, 6
- Huterer, D. & Cooray, A. 2005, *Phys. Rev. D*, 71, 023506
- Lewis, A. & Bridle, S. 2002, *Phys. Rev. D*, 66, 103511; See also the CosmoMC website at:  
<http://cosmologist.info>.

- Li, H., Su, M., Fan, Z. H., Dai, Z. G. & Zhang, X. 2008, *Phys. Lett. B*, 658, 95
- Lloyd-Ronning, N. M. & Ramirez-Ruiz, E. 2002, *ApJ*, 576, 101
- Miknaitis, G., et al. 2007, *ApJ*, 666, 674
- Norris, J. P., Marani, G. F. & Bonnell, J. T. 2000, *ApJ*, 534, 248
- Riess, A. G., et al. 2007, *ApJ*, 659, 98
- Schaefer, B. E. 2007, *ApJ*, 660, 16
- Spergel, D. N., et al. 2007, *ApJS*, 170, 377
- Su, M., Li, H., Fan, Z. H. & Liu, B. 2006, arXiv:astro-ph/0611155
- Tegmark, M., et al. 2004, *Phys. Rev. D*, 69, 103501
- Tegmark, M., et al. 2006, *Phys. Rev. D*, 74, 123507
- Wang, F. Y., Dai, Z. G. & Zhu, Z. H. 2007, *ApJ*, 667, 1
- Wang, Y. & Mukherjee, P. 2006, *ApJ*, 650, 1
- Wright, E. 2007, *ApJ*, 664, 633
- Xia, J. Q., Zhao, G. B., Feng, B., Li, H. & Zhang, X. 2006, *Phys. Rev. D*, 73, 063521
- Xu, D., Dai, Z. G. & Liang, E. W. 2005, *ApJ*, 633, 603
- Zhang, X. F., Li, H., Piao, Y. S. & Zhang, X. 2006, *Mod. Phys. Lett. A*, 21, 231
- Zhao, G. B., Xia, J. Q., Li, M., Feng, B. & Zhang, X. 2005, *Phys. Rev. D*, 72, 123515
- Zhao, G. B., et al. 2007a, *Int. J. Mod. Phys. D*, 16, 1229
- Zhao, G. B., et al. 2007b, *Phys. Lett. B*, 648, 8